Helanto, Karoliina; Talja, Riku; Rojas, Orlando J.

Talc reinforcement of polylactide and biodegradable polyester blends via injection-molding and pilot-scale film extrusion

Published in:
Journal of Applied Polymer Science

DOI:
10.1002/app.51225

Published: 05/11/2021

Document Version
Publisher's PDF, also known as Version of record

Received: 26 November 2020 | Revised: 6 May 2021 | Accepted: 24 May 2021

DOI: 10.1002/app.51225

ARTICLE

Applied Polymer SCIENCE WILEY

Talc reinforcement of polylactide and biodegradable polyester blends via injection-molding and pilot-scale film extrusion

Karoliina Helanto[1,2] | **Riku Talja**[2] | **Orlando J. Rojas**[1,3]

[1]Department of Bioproducts and Biosystems, School of Chemical Engineering, Aalto University, Espoo, Finland

[2]Metsä Board Corporation, Espoo, Finland

[3]Bioproducts Institute, Departments of Chemical & Biological Engineering, Chemistry, and Wood Science, The University of British Columbia, Vancouver, Canada

Correspondence
Karoliina Helanto, Department of Bioproducts and Biosystems, School of Chemical Engineering, Aalto University, P.O. Box 16300, FI-00076 Aalto, Espoo, Finland,.
Email: karoliina.helanto@aalto.fi

Abstract

As a renewable and biodegradable polymer, polylactide (PLA) has taken a foothold in the packaging industry. However, the thermomechanical and barrier properties of PLA-based films need to be improved to facilitate a wider adoption. To address this challenge, we examined the effect of talc reinforcement in composites based on PLA and a biodegradable polyester. Masterbatches of the polymers and talc were produced by melt compounding and processed by either injection-molding or film extrusion in a pilot-scale unit operating at 60–80 m/min. The effect of talc was investigated in relation to the morphological, thermal, mechanical, and barrier properties of the composites. Based on SEM-imaging, talc was found to increase the miscibility of PLA and the polyester while acting as a nucleating agent that improved PLA crystallinity. While this effect did not track with an increased mechanical strength, the composites with 3–4 wt% talc displayed a significantly higher barrier to water vapor. Compared to the neat polymer films, a reduction of water vapor transmission rate, by ~34–37%, was observed at 23°C/50% RH. Meanwhile, the systems loaded with 1 wt% talc showed a reduction in oxygen transmission rates, by up to 34%. Our results highlight the challenges and prospects of commercial PLA-based blends filled with talc from films extruded in pilot-scale units.

KEYWORDS

biodegradable, biopolymers and renewable polymers, composites, extrusion, films

1 | INTRODUCTION

The packaging industry is constantly developing materials to ensure better performance and sustainably while meeting regulatory specifications.[1,2] Packaging materials are selected and combined to fulfill the end-use requirements.[3] Currently, the packaging industry is the largest sector utilizing plastics. The most common polymers used for packaging are polyethylene (PE), polypropylene (PP), polyethylene terephthalate (PET), polystyrene (PS), and polyvinyl chloride (PVC).[4,5] Meanwhile, the development and utilization of renewable raw materials in packaging solutions are gaining importance.[3] PLA, as a renewable and biodegradable polymer, has become an alternative for petroleum-based polymers. Nevertheless, the low heat resistance, brittleness, low crystallinity, and

modest barrier properties of PLA have limited its use.[3,6–9] In order to improve PLA film properties, flexible polymers, plasticizers, fillers and nucleating agents have been considered.[7–9] PLA has been blended, for example, with poly(butylene adipate-co-terephthalate) (PBAT),[8,10] poly(e-caprolactone) (PCL),[8,11] poly(ethylene glycol) (PEG),[9,11] poly(propylene glycol), poly(trimethylene carbonate) (PTMC)[11] and triphenyl phosphate,[9] altering the physicochemical properties, crystallinity, viscoelasticity, processability and overall end-product performance. Likewise, fillers such as talc, kaolin, calcium carbonate, and mica have been incorporated for enhancing the mechanical, thermal, and barrier properties while reducing the cost.[12] Talc ($Mg_3Si_4O_{10}[OH]_2$) is extensively studied, in part, owing to its neutral charged and hydrophobicity as well for its suitability as a nucleating agent in polymer matrices.[13] Talc has a special three-layered structure held together by weak van der Waals forces[14] and with the outermost layer comprising tetrahedral silica sheets next to octahedral brucite. Talc's structure and softness enable it as a filler that can be dispersed under shear, enhancing the properties of polymer/filler composites.[12,13,15] Among the factors effecting the properties of composites one can include aspect ratio, concentration, filler orientation, and adhesion to the polymer matrix.[12]

PLA/talc composites have been studied and significant improvement has been achieved. The most common finding has been the increased crystallization based on the nucleating effect of talc.[9,13,15–18] Also, with a smaller particle size, talc has been shown to produce better crystallinity development.[19,20] Talc has been observed to reinforce and toughen PLA at loadings as high as 30 wt%.[13,18] Used in minor amounts, talc has been reported to improve puncture resistance, which is an important feature of packaging films.[17] Also, at lower addition (1 wt%), talc has been reported to work as a lubricant and to decrease the viscosity of PLA melts.[18] Talc also improves miscibility of polymer blends and the thermal stability of the composite. Such effects have been explained to be the result of a decreased permeability, causing blockage of the volatile decomposition compounds.[21] For example, an immiscible blend, PLA/poly(e-caprolactone) (PCL), was effectively compatibilized considering PLA domains in the surrounding PLC polymer matrix. The enhanced miscibility was explained by the reduced size of the PLA domains and voids in the matrix and by the improved inter-polymer adhesion. Meanwhile, as a consequence of the latter effect, the barrier properties were improved as well.[22] For example, compared to neat PLA, solvent cast PLA/talc films (talc content of 5–15 wt%) displayed a better barrier to water vapor (up to 55% improvement). Similarly, oxygen permeability is also reduced with talc addition. Compared to neat PLA, a moderate reduction was achieved at 2 wt% talc addition[23] and a more substantial effect (reduction by ~50%) was noted at 1–3 wt% talc loading in PLA/poly(trimethylene carbonate) (PTMC) composites.[11] The main factors that contribute to the benefits of talc addition, when well dispersed in the matrix, include the increased crystallinity and the torturous structure it forms.[17]

There are several processes to manufacture PLA-based films for packaging. This includes extrusion coating, in which a PLA is applied onto a base material, such as paper. Currently, the prevalent application consists of PE coatings on paper, typically used in food service products.[24] Therefore, the aim of the present work was to investigate the potential of talc to improve PLA-based materials and, most significantly, to find a more sustainable option for conventional petrochemical-based packaging materials produced by extrusion coating. We examined the effect of talc (non-surface-treated) on the morphological, thermal, mechanical, and barrier properties of films produced with blends of commercial PLA and biodegradable polyesters. Melt-compounded masterbatches were extruded into films and injection-molded into specimens for testing. As an evolution of extrusion coating of PLA,[24–27] talc has been incorporated in PLA to produce composite PLA/talc films. So far, this has been achieved by using compression molding,[21,23] solvent casting,[11,17] extrusion film-blowing[6,12,15] and extrusion casting.[28] Differentiating from this earlier work, we produced PLA/talc films by using a pilot-scale extrusion coating unit which endowed films with significantly smaller thicknesses (18–26 μm).

2 | EXPERIMENTAL

2.1 | Materials

Two commercial PLA/biodegradable polyester blends were used in this study, Ecovio® PS 1606 (BASF) and Mater-Bi® EX51A0 (Novamont S.p.A.), hereafter referred to as "PLA1" and "PLA2", respectively. PLA1 density was 1.24–1.26 g/cm^3 (ISO 1183) and the shore D hardness was 71 (ISO 868). PLA1 melt volume rate (190°C, 2.16 kg, ISO 1133) was 18–42 mL/10 min, and the vicat VST A/50 (ISO 306) was 61°C. For PLA2 the density was 1.24 g/cm^3 (ASTM D792) and melt flow rate (190°C, 2.16 kg, ISO 1133-1) was 9 g/10 min. The talc (Finntalc M03N, median particle size 1 μm) was sourced from Mondo Minerals. The samples are referred to according to the following nomenclature: Polymer blend (PLA1 or PLA2)/talc content (wt%) specimen type "i" or "f", where "i" refers to samples obtained by injection molding, and "f" refers to extruded film samples. For example, the test specimen "PLA1/3i" indicates injection molded samples obtained from PLA1 with 3 wt% talc loading.

2.2 | Compounding

Masterbatches were prepared with the polymer blend (70 wt%) and talc (30 wt%) (PLA1/30 or PLA2/30) using a 25 mm Coperion ZSK 26 Mc counter-rotating twin-screw extruder, 32 L/D ratios with K-Tron gravimetric feeder K-ML-KT20. The temperature profile of the extruder, from the feeding to die zone was 195/195/185/180/175/170/165/160°C and the applied screw speed was 350 rpm with a yield of 30 kg/h for both of the masterbatches. The extruded filaments were cooled in 20°C water and air and finally pelletized. The talc content was determined from the residual ash (925°C) and the results are listed in the supporting information (Table S1).

2.3 | Injection-molding

Standard tensile strength (ISO 527-2/1A) and impact strength (ISO 179-1/1e) specimens were prepared by injection-molding with an Engel ES 200/40 injection-molding machine (D = 25 mm). The temperature profile of the screw from the feeding to the nozzle zone was 185/200/210/220°C, with packing pressure of 30 bar and packing pressure time of 20 s. The applied Injection distance and injection speed were 70 mm and 150 mm/s, respectively. The mold temperature and cooling time were set at 30°C and 30 s, respectively.

2.4 | Film extrusion

Film extrusion was carried out in a pilot extrusion coating line (D = 60 mm, L/D = 30) with a T-die (deckles of 590 mm). The polymers and the masterbatches were dried at 45–50°C for 20 h before extrusion. The polymer and masterbatch pellets were mixed in a 100-L container resulting in the given talc content prior to film extrusion. The temperatures of the extruder from the feeding to the die zone corresponded to 170/195/210/230°C (PLA1) and 219/240/255/265°C (PLA2) using 80 rpm, back pressure of 87–96 bar, air gap of 160 mm and nip pressure of 6 bar. Chill roll type was glossy and the temperature was 20°C. The films were extruded on silicon paper sheets in order to prevent adhesion between the film and base material.

2.5 | Characterization

2.5.1 | Morphology

Injection-molded specimens (ISO 527-2/1A) were cooled with liquid nitrogen for 5 min and then fractured in half. The fracture surface was imaged with a scanning electron microscope (SEM, Jeol JCL-6000Plus) under high-vacuum with secondary electron detector (SED). The analyzed fracture surfaces were sputtered with a gold layer.

2.5.2 | Thermal characteristics

Differential Scanning Calorimetry (DSC) measurements were carried out with a Thermal Analyzer (DSC Q2000) under nitrogen atmosphere at a flow rate of 50 ml/min. The samples, granules and injection- molded specimens, were weighted (5–10 mg) and placed in aluminum pans and heated from 20 to 200°C at a constant heating rate of 10°C/min (with holding at 200°C for 2 min). Thereafter, the samples were cooled to 20°C at a constant cooling rate of 20°C/min and reheated to 200°C at a heating rate of 10°C/min. The glass transition (T_g), crystallization (T_c), and melting (T_m) temperatures of the composites were determined using the thermograms. Equation 1 was used to calculate the apparent degree of crystallinity of the composites, X_c:

$$X_C(\%) = 100\frac{\Delta H_m - \Delta H_C}{\Delta H_0 W_{PLA}} \quad (1)$$

where ΔH_m and ΔH_C are the melting and crystallization enthalpy upon heating and W_{PLA} is the weight fraction of the PLA in the samples. ΔH_0 is the melting enthalpy of 100% crystalline PLA (assumed to be 93 J/g).[7,12,20,29]

The thermal stability of the granulates and injection-molded samples (4.2–7.7 mg) were studied by TGA (8000™ Thermogravimetric Analyzer, PerkinElmer). The samples were placed in ceramic pans and the analysis was carried out using a nitrogen gas purge of 20 ml/min at heating from 27 to 950°C at a rate of 10°C/min.

2.5.3 | Mechanical properties

Tensile and elongational properties were determined by Zwick Roell Z010 material tester (max load 10kN) according to ISO 527-2:2012 under standard conditions (23 ± 2°C and 50 ± 10% RH). Tests were carried out both for the injection molded specimens and films, which were cut into shape according to ISO 527-2/1A. A preliminary crosshead separation of 110 mm and a crosshead speed of 5 mm/min were used. Five replicate measurements were conducted for each sample and an average was reported. The impact strength (Charpy edgewise impact with single-notched specimen) was determined with a Zwick impact tester with 1 J hammer according to ISO 179 under standard conditions (23 ± 2°C and 50 ± 10% RH). A notch was prepared with Ray–Ran politest

motorized notching cutter. Both, the tensile and impact strength test specimens were conditioned for at least 88 h according to ISO 291 at 23°C and RH 50%.

2.5.4 | Barrier characteristics

The water vapor transmission rate (WVTR) was determined from extruded films according to modified ISO 2528 standard. The weight change of the cup filled with desiccant (anhydrous $CaCl_2$) and covered with test specimen was followed as a function of time. The test was implemented in alternating climate chamber (BINDER, model KMF 240) at 23°C and 50% RH and 38°C and 90% RH. Two parallel measurements were performed except for the samples corresponding to PLA1 (3 wt%) and PLA2 (3 wt% and 4 wt%) which presented pinholes and therefore did not produce reliable results. The

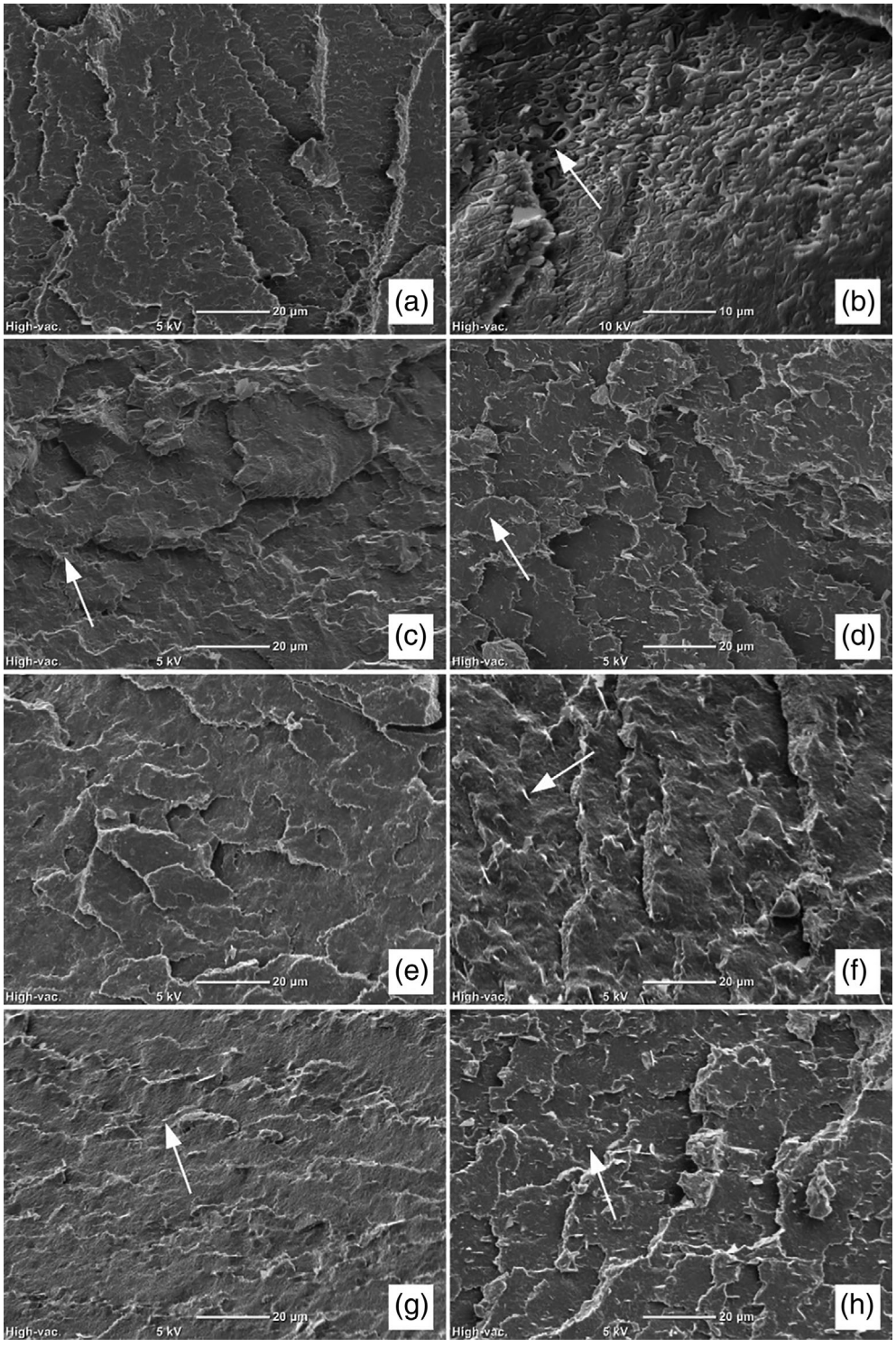

FIGURE 1 SEM images the fractured surfaces of injection-molded specimens of (a) neat PLA1/0i, (b) PLA1/2i, (c) PLA1/3i, (d) PLA1/5i, (e) PLA2/0i, (f) PLA2/3i, (g) PLA2/4i, and (h) PLA2/5i. The magnification used in the images were x1000, except for image (b), x2000

oxygen transmission rate (OTR) of the extruded films was determined at 23°C and 50% RH with an oxygen transmission rate analyzer (MOCON Ox-Tran 2/21 MH/SS) according to ASTM D3985-05. Two parallel measurements were performed and an average was reported. The results of WVTR and OTR have been normalized by the film thicknesses.

3 | RESULTS AND DISCUSSION

3.1 | Morphology

The fracture surfaces of injection-molded specimens (PLA1 and PLA2) are presented in Figure 1, noting that some stretching occurred during fracture of the neat polymer and low talc content samples (Figure 1(a,b,e)). The areas after elastic recovery can be seen as rolled and curly edges with light gray color (Figure 1(a,e)) while creep can be detected in Figure 1(b). The main observations that can be derived from the SEM images include the miscibility of the polymer matrix and the orientation of the talc particles. The compatibility of the polymers seemed to improve with talc addition. For instance, for neat PLA1 (Figure 1(a)) and PLA2 (Figure 1(e)) samples, polyester particles were seen; similar particles were apparent in PLA1/1i and PLA1/2i (Figure 1(b)) and in PLA2/1i (Figure S1, supporting information), PLA2/2i and PLA2/3i (Figure 1(f)). Although the immiscibility is more clearly seen in the SEM images of PLA1in Figure 1, the same phenomenon was also observed for PLA2 (Figure 1 and Figure S1). Similarly, phase-separated features have been reported for PLA/PBAT blends[30–32] and explained by the poor interfacial adhesion between PLA and PBAT.[30,31] Micro- and nanosized talc particles have been used to improve the compatibility of immiscible blends of polypropylene (PP) and polyamide (PA6). Nanosized talc reduced extensively the domain size and therefore enhanced the morphology of the blends. Natural, microscaled talc has been reported to reduce the domain size by the Zhu's mechanism, which is based on the cutting effect of clay under the shear of mixing.[33] In the present study, a better compatibility was observed with talc addition of >2 wt% in PLA1 (Figure 1(c,d)). Similarly, for PLA2, talc addition >3 wt% was effective in reducing phase-separation (Figure G and H). The mechanism explaining the reduced domain size and thereby improved morphology of the composites involves Zhu's hypothesis[34] based on the nature and the particle size of the used talc.

The talc particles seemed to settle mainly in the mold fill direction, which can be seen most clearly in Figure 1 (d,h). Filler dispersion appeared uniform throughout the fracture surface and showed no observable agglomeration. Since the masterbatches were processed under thorough mixing conditions in the twin-screw extruder while the injection molded specimens underwent less effective mixing in the single-screw injection-molding machine, the injection molded specimens can be classified as being both partly distributively and dispersively mixed.[35] Talc particles in injection-molded samples have been reported to settle differently in the skin and core regions. In the skin region, the filler particles have been observed to align in the mold fill direction, and less favorably in the core region.[36] In this study, no significant differences in talc orientation were observed in the skin and core regions resulting in uniform morphology and behavior in testing. Strong filler-matrix interactions can be proposed based in the tightly embedded talc particles[37] seen in the fractured surfaces in Figure 1(d,h).

As far as the extruded films, we note that sample preparation for cross section imaging was challenging due to the nature of the thin films. Talc particles were observed to orient parallel to the film surface, as observed in typical polymer processing for packaging materials.[38] SEM images of the film surfaces indicated some pinholes at a higher talc loading, for both polymer blends, PLA1 and PLA2. An example is presented in Figure S2. Few pinholes were observed in SEM images of PLA1 films with 3–5 wt% of talc while a higher talc concentration (4 wt%) was needed for pinhole formation in PLA2 films. Naturally, pinholes exert a negative effect in the barrier,[39] and mechanical properties.

3.2 | Thermal characteristics

The main thermal properties of the composites obtained from the second heating cycle in DSC and TGA thermograms are presented in Table 1.The second heating cycle of DSC was used for comparison given that the samples tested underwent different thermal history; however, the results of the first heating cycle are provided as a reference in the supporting information (Table S1). As expected, the addition of talc did not significantly affect the T_g of the respective system. Changes were noted in the T_c and in the X_c. T_c decreased and X_c increased with talc loading, which indicates the effect of the filler as nucleating agent. Also, the decreasing trend of ΔH_c is a result of the nucleating effect of talc in the cooling cycle. Similar DSC behavior has been reported for PLA/talc composites,[7,15,16] where talc has been proposed to accelerate polymer crystallization due to its strong nucleating effect.[11,16,17] Except for two samples (PLA1/2 and PLA2/4), compared to the previous talc loading, the crystallinity decreased in the range of miscibility for both

TABLE 1 Thermal properties of biopolymer/talc composites. ΔH values are presented only for the polymer fraction. The measurements were conducted with polymer granules (PLA1/0, PLA2/0), injection molded specimens (sample points with 1–5 wt% of talc), and masterbatches (PLA1/30, PLA2/30)

Polymer/talc wt%	T_g (°C)	T_c (°C)	T_m (°C)	ΔH_c (J/g)	ΔH_m (J/g)	X_c (%)	T_5 (°C)	T_{50} (°C)
PLA1/0	62.1	104.5	169.8	17.2	23.5	6.8	335.4	382.8
PLA1/1i	60.6	93.5	167.4	9.1	26.2	18.4	332.2	381.0
PLA1/2i	61.2	94.8	167.3	11.7	25.4	14.7	335.2	378.5
PLA1/3i	60.9	93.2	167.5	6.8	25.3	19.9	329.9	367.9
PLA1/4i	60.2	93.2	167.8	6.7	25.1	19.8	332.9	381.9
PLA1/5i	60.8	93.2	167.7	4.3	24.8	22.0	328.7	381.6
PLA1/30	62.1	95.0	168.9	1.1	25.6	26.3		
PLA2/0	61.6	106.4	168.4	19.0	24.7	6.2	331.1	372.6
PLA2/1i	61.1	98.2	166.9	15.6	25.6	10.8	335.2	375.6
PLA2/2i	61.3	96.0	166.9	14.1	24.4	11.1	340.3	377.2
PLA2/3i	60.8	95.0	166.7	12.3	26.3	15.0	336.4	376.6
PLA2/4i	61.6	95.9	166.7	11.8	23.7	12.8	339.5	379.4
PLA2/5i	61.3	94.7	166.7	10.6	24.7	15.2	339.7	377.1
PLA2/30	61.9	96.7	167.6	4.5	23.9	20.8		

PLA1 and PLA2 composites. The immiscibility of a polymer blend strongly influences the crystallization of the polymer in the matrix. The crystallization of an immiscible blend is expected to occur in multiple crystallization events, at different temperatures.[40] Here, the changes in miscibility at given talc loading correlated with the change of crystallinity.

A single melting peak has been reported for neat PLA but two peaks are expected for PLA/talc composites.[7,17] Neat PLA appears in the α crystalline form[17] while the composites are divided into less thermally stable β crystalline and to α crystalline forms.[7,17] The double melting peaks of neat PLA and its composites are often the result of recrystallization, which occur during the slow crystallization process.[17,32] In the DSC thermograms, some traces of double melting peaks are observed (thermogram C in Figure 2); however, such peaks are not as distinctive as presented in the literature, possibly due to the low talc loading.

The decomposition temperatures (5% [T_5] and 50% [T_{50}]) presented in Table 1, indicate that no significant degradation took place during melt processing since such values are higher than the processing temperature (during extrusion, the temperatures measured on the composites were between 241–272°C). The TGA analyses were carried out under nitrogen atmosphere, which is different than that of the extrusion process (air). We note that a lower decomposition temperature is expected in air but comparison across samples is simplified under a more inert atmosphere (for a discussion about the different thermal decomposition in nitrogen and air, the readers is referred to Xiang *et al.*[41]). The losses at T_5 of the plain polymers were close to the T_5 of pure PLA, which is reported to be 334.7 under nitrogen atmosphere (10°C/min heating rate).[41] T_5 of PLA1 samples decreased moderately and T_{50} decreased at lower talc additions and increased back to the same level at higher talc content. A moderately increasing trend for T_5 and T_{50} was observed in PLA2 samples. An increase of thermal stability was

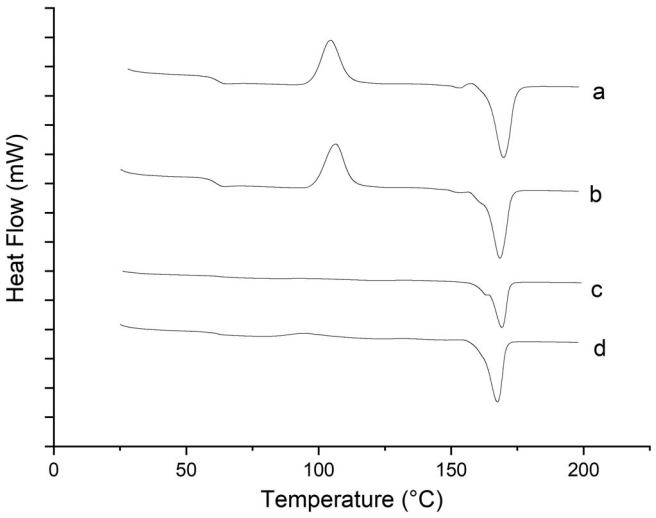

FIGURE 2 Thermograms from the second DSC heating cycle: a, PLA1; b, PLA2; c, PLA1/30; and d, PLA2/30. The position of the thermograms have been shifted in order to compare the results in a single figure. Tick value is 2 mW

TABLE 2 Mechanical properties of biopolymer/talc composites in injection-molded ("i") and film ("f") form

Polymer/talc wt%	TS (MPa)	TS at break (MPa)	dL at break (%)	E Modulus (Mpa)	Impact strength (kJ/m2)
PLA1/0i	28.8 ± 0.1	1.8 ± 0.6	15.3 ± 1.6	1550 ± 7	57.7 ± 3.9
PLA1/1i	27.3 ± 0.5	5.9 ± 3.7	5.2 ± 1.4	1529 ± 15	59.0 ± 3.4
PLA1/2i	28.1 ± 0.1	1.4 ± 0.0	9.8 ± 0.8	1536 ± 8	
PLA1/3i	27.2 ± 0.1	7.9 ± 1.4	5.5 ± 0.5	1542 ± 29	
PLA1/4i	28.4 ± 0.4	2.1 ± 0.7	11.6 ± 1.3	1583 ± 20	
PLA1/5i	26.6 ± 0.2	10.5 ± 0.5	4.5 ± 0.6	1534 ± 30	58.9 ± 3.7
PLA2/0i	36.6 ± 0.5	29.4 ± 1.7	288.3 ± 24.0	1789 ± 16	81.7 ± 8.6
PLA2/1i	35.9 ± 0.4	29.0 ± 1.7	289.7 ± 25.4	1749 ± 17	73.1 ± 3.8
PLA2/2i	36.0 ± 0.2	30.9 ± 1.7	307.3 ± 21.6	1792 ± 22	
PLA2/3i	35.4 ± 0.3	32.7 ± 1.0	327.3 ± 17.4	1785 ± 38	
PLA2/4i	35.3 ± 1.0	30.2 ± 0.9	311.1 ± 20.9	1787 ± 30	
PLA2/ 5i	35.5 ± 0.3	28.4 ± 1.7	295.4 ± 18.2	1804 ± 9	65.2 ± 3.5
PLA1/0f	30.9 ± 6.6	11.3 ± 1.4	2.3 ± 0.1	2120 ± 416	
PLA1/1f	24.8 ± 1.1	10.8 ± 0.9	1.9 ± 0.1	1783 ± 79	
PLA1/2f	20.6 ± 1.8	9.1 ± 0.8	1.6 ± 0.1	1629 ± 114	
PLA1/3f	16.4 ± 2.2	6.9 ± 0.9	1.3 ± 0.1	1543 ± 162	
PLA1/5f	13.0 ± 3.0	5.0 ± 1.6	1.1 ± 0.2	1518 ± 323	
PLA2/0f	29.1 ± 1.8	10.4 ± 1.6	3.2 ± 0.3	1919 ± 128	
PLA2/1f	27.0 ± 1.5	9.3 ± 2.6	2.4 ± 0.3	1824 ± 105	
PLA2/3f	27.3 ± 1.6	11.4 ± 1.1	2.0 ± 0.1	1908 ± 74	
PLA2/4f	27.5 ± 1.8	12.0 ± 0.7	2.0 ± 0.1	1925 ± 85	

expected due to the reported effect of talc, which weakens the permeability and therefore prevents the out-diffusion of the volatile compounds that evolve during decomposition.[21] The miscibility of the composites changed at 2–4 wt% talc loadings, which likely explains the dip observed in the TGA profile at 2–3 wt% talc loading.

3.3 | Mechanical properties

3.3.1 | Tensile strength and elongation

Tensile strength (TS) and elongational properties were analyzed for both, the injection-molded and the extruded film specimens (Table 2). The addition of talc increased the crystallinity of the polymers while, based on the literature, the tensile strength should increase until reaching an optimum at a given filler content, where intermolecular bonding occurs in the crystalline phase.[42] However, in our samples, under the conditions of processing used, the tensile strength remained somewhat similar for the injection-molded samples. Meanwhile, the tensile strength of PLA1 was reduced upon talc addition. Among the intermolecular bonding, other multiple factors influence the tensile strength of polymer/filler composites, such as the interactions between polymers and fillers, filler-filler interactions, and orientation of the filler in the composite structure.[36] In addition, the film extrusion process affects the orientation of the films for example, polymer melt draw ratio, air gap, and machine speed.[43] The likely cause for the reduced tensile strength of PLA1 films related to the brittle nature of the polymer and the interactions between the polymer matrix and talc, as seen in elongation results (Figure 3).

PLA1 and PLA2 polymers differed from each other significantly in their elongational properties (Figure 3). PLA2 shows elastic behavior with strain hardening while PLA1 was rather hard and brittle. In addition, their behavior after talc addition differed in the injection-molded samples. The elongation was not reduced in PLA2 samples whereas PLA1 samples displayed a decreasing trend upon talc addition. However, PLA1/2i and PLA1/4i stood out for their higher elongation. Similarly, PLA2/3i had the highest elongation among the PLA2 samples. The range where the elongation was the highest among the composites is close to the observed

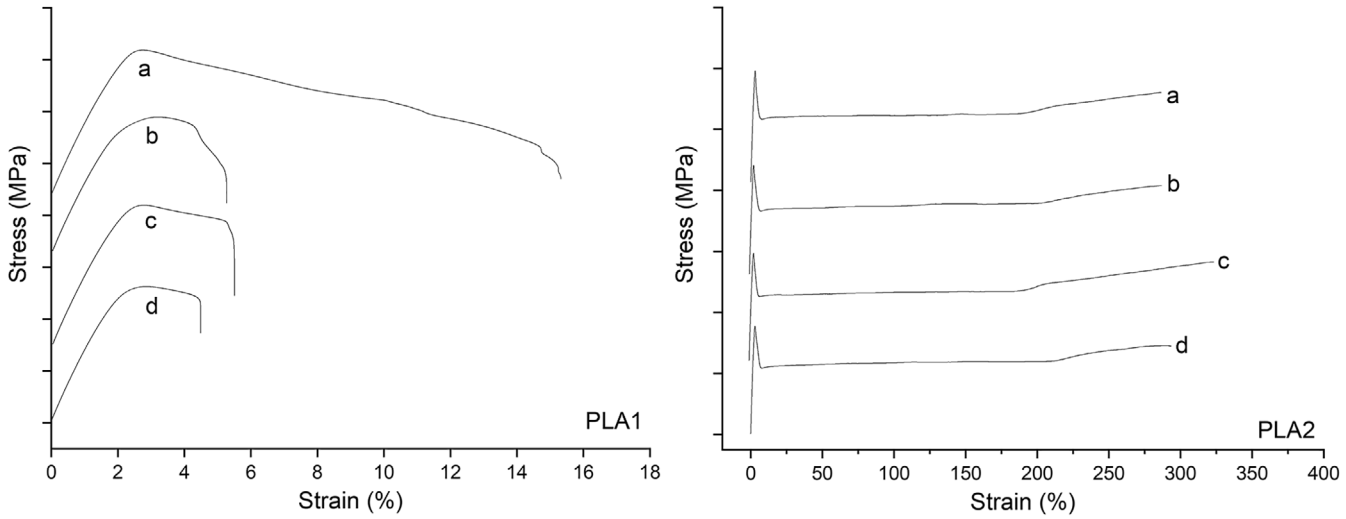

FIGURE 3 Stress–strain curves of the injection-molded composites: a, neat; b, 1 wt%; c, 3 wt%; and d, 5 wt% talc addition. The position of the curves have been shifted in order to compare the results in a single figure. Tick values are 10 MPa in PLA1 and 20 MPa in PLA2

change in the compatibility of the polymer matrices. The decrease in elongation could be explained by the higher filler loading, which leads to areas of stress concentration and causes cracking.[20] Likely, and for the same reason, a decrease in elongation after talc was detected in the films prepared from both polymers. The elastic modulus of the composites was mainly lower than the neat polymer but an increasing trend was observed from PLA1/1i to PLA1/PLA1/4i. One clear improvement (PLA1/4i) compared to the neat polymer was detected. Similar development of elastic modulus in PLA/talc composites have been reported before. Increased elastic modulus has been explained by the stress transfer from the polymer matrix to the talc particle.[21]

3.3.2 | Impact Strength

Talc addition did not have major effects on PLA1 impact strength but for PLA2 a reduction was noted (Table 2). The reduction in impact strength has been reported to relate to the increased crystallinity and decreased elongation.[20] Accordingly, compared to PLA2, PLA1 should show a change in impact strength with talc loading, given the increased crystallinity after talc addition (first heating cycle, Table S1) and more limited elongation. However, PLA2 presented a relatively higher impact strength with talc addition. One can hypothesize that as the talc particles become smaller, the impact strength is reduced.[20] It has also be noted that the adhesion between the filler and the polymer matrix has a direct influence on impact strength.[37] PLA1 polymer matrix possibly presented

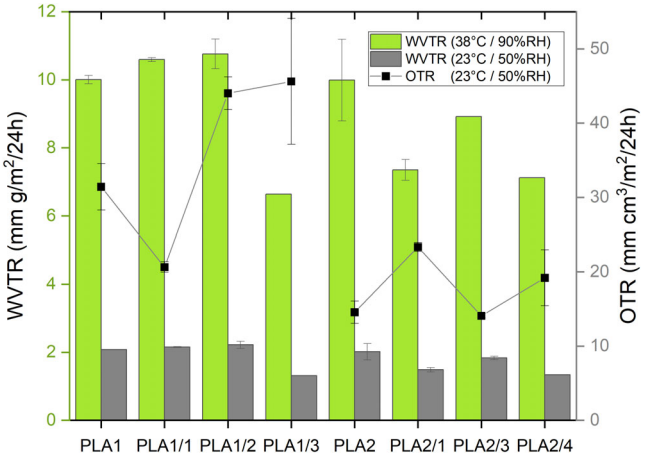

FIGURE 4 Barrier properties (WVTR & OTR) of biopolymer/talc (wt%) composite films. The results have been normalized by the film thicknesses [Color figure can be viewed at wileyonlinelibrary.com]

better adhesion with talc particles; together with the somewhat higher miscibility, these are reasons that explain the different behavior in impact strength.

3.4 | Barrier properties

Water vapor and oxygen resistances are desired properties for packaging materials, especially in food packaging.[4,11,17,23] The barrier properties were measured for films with a thickness between 18 and 26 μm. The presence of talc reduced WVTR for PLA1 at 3 wt% and PLA2 at all talc loadings (Figure 4). As seen, the testing

conditions have a major effect on WVTR but the trends are maintained.[22] A significant decrease in both conditions (23°C/ 50% RH and 38°C/ 90% RH) was observed in PLA1/3f, and in PLA2/1f and PLA2/4f samples. In this study, the WVTR (23°C/50% RH) for PLA1 and PLA2 improved by 34–37% with the addition of 3–4 wt% talc. In comparison, the WVTR of solvent casted PLA/talc films was reduced by 55% at a high talc content, 15 wt%.[17] On the other hand, the WVTR of solvent casted PLA/PTMC films was improved by 25% after 2 wt% talc addition.[11] In compression molded PLA/PCL/talc sheets the WVTR decreased, up to 25%, with 3 wt% talc.[22] Considering the amount of talc used in this study, the WVTR improvements achieved were comparatively high. While solvent casting and compression molding have been applied for PLA/talc composite films, a distinctive feature of our work is the use of a pilot-scale extrusion coating line operated at relatively high speed (60–80 m/min).

Overall, the improvement of WVTR caused by talc addition can be explained by several factors. Talc increases the crystallinity and the tortuosity of the films.[17] In addition, talc promotes the hydrophobicity and density of polymer films leading to a more limited water diffusion rate.[11] Remarkably, the notable improvement in water barrier effect took place at the same conditions that led to a better polymer compatibility. In this study, an optimum talc content was not identified as far as WVTR. Similar to the injection molded specimens, the mixing of the masterbatches and the neat polymers in the film extrusion process were executed with single-screw extruder, which is not as effective mixer as the twin-screw extruder. Thus, it is reasonable to state that the distribution of the talc particles in the films can be further improved.

The OTR was observed to improve, by 34%, with 1 wt % talc additions in PLA1 films but with higher talc loading, a reverse effect was observed. PLA2 polymer behaved differently. A small amount of talc reduced the oxygen barrier, whereas the OTR was improved marginally, by 3.3% with 3 wt% talc. According to these results, the optimum talc content as far as OTR, is 1 wt% for PLA1 and 3 wt% for PLA2. The behavior of PLA1 at low talc content could be explained by the good distribution of talc particles and by the increased crystallinity, while the increased OTR after 2–3 wt% talc addition is likely caused by agglomerates. Interestingly, at PLA1/3f presented the lowest WVTR and the highest OTR. This could be explained by the hydrophobic nature of talc and the polar water molecules. The penetration of oxygen molecules through hydrophobic talc agglomerates can be easier, given the nonpolar nature of the system compared to water molecules. PLA2 kept somewhat the same OTR level with PLA2/3, whereas the OTR was increased by 32% with PLA2/3. PLA2/1f was the exception, with a higher OTR than the rest (60% higher than that of neat PLA2). As seen in the injection molded samples, the immiscibility of the PLA2 talc blends took place at lower talc content (Figure 1) together with the observation of moderate increase in crystallinity (Table 1), and similar behavior in films could explain the results. However, defects that were not detectable could also be a possible explanation for the results. The significantly improved OTR after 3 wt% talc addition has been reported by other authors: OTR of solvent casted PLA/PTMC/talc film was reduced by 50%,[11] while the OTR of compression molded PLA/PCL/talc sheets decreased by 33%,[22] and in PLA/ talc extrusion blown films a 30% reduction was obtained.[15]

PLA (175 cm^3/m^2 d bar in 23°C/50% RH) has a lower OTR compared with LDPE (2000 cm^3/m^2 d bar in 23°C/50% RH) but much higher than ethylene-vinyl alcohol (EVOH, 27 mol %) (0.04 cm^3/m^2 d bar in 23°C/50% RH), which is considered to be an oxygen barrier material. As far as the water vapor barrier, PLA (22 g/m^2 d in 23°C/85% RH) has been reported to be less preferred than LDPE (0.9 g/m^2 d in 23°C/85% RH) and EVOH (27 mol %) (3.2 g/m^2 d in 23°C/85% RH).[44] Gas and vapor permeability of polymer composites are affected by multiple factors. The solubility of the gas or vapor into the polymer, the size of a gas molecule compared to the gaps in the polymer matrix, and the testing conditions, all of which are key features in permeability rating. The filler has an effect on its own, depending on aspect ratio, orientation, dispersion, and shape. Filler volume, density, compatibility, and crystallinity of the matrix have also a great influence on the barrier properties.[45] The probability of molecular diffusion is higher in amorphous polymers compared to that in dense crystalline regions.[17,39,45] The permeability properties are also affected by defects such as pinholes and microvoids.[39]

4 | CONCLUSIONS

Composites were produced by melt compounding followed by injection-molding or film extrusion. To this end, commercial PLA/biodegradable polyester blends were mixed with talc at different loadings (0–5 wt%). According to SEM analyses, a reduction in the characteristic domain size and phase-separation was observed with talc addition (PLA1/3i and PLA2/4i). As seen from the SEM images, talc particles settled mainly in the melt flow direction and parallel to the injection-molded and film extruded surfaces to maximize the tortuosity of the matrix. At higher talc contents, some agglomerations and pinholes were detected in the SEM images of the films. Talc acted as a nucleating agent in the composites and

increased the degree of crystallinity. Talc did not improve the tensile strength nor elongation while the impact strength of PLA1 remained at the same level after talc addition (meanwhile, PLA2 samples experienced a drop). However, the elastic modulus was improved with PLA1/4i, PLA2/2i, and PLA2/5i samples. Significant improvement in the barrier properties was observed, by 34–37% for WVTR (23°C/50% RH) for both polymers. OTR was improved by 34% with talc addition (1 wt%) in PLA1 films (by 3.3% in PLA2/3f).

The notable benefit of the talc addition to commercial PLA/biodegradable polyester blends was observed in terms of a better compatibility and the barrier properties. These properties are most relevant in packaging. Together with the renewability and the biodegradability of the presented system, our results offer excellent prospects for PLA-based barriers, as shown in pilot condition, which can be scale up to larger capacities. Polymer filler interactions should be enhanced in order to improve the mechanical properties. Other filler types can be considered in future studies.

ACKNOWLEDGMENTS

The authors wish to thank Arctic Biomaterials Oy for the compounding of the masterbatches, the assistance of Sai Li with the preparation of injection-molded specimens, and Laura Koskinen for the help with the figures. The research group of Paper Converting and Packaging Technology at Tampere University was gratefully acknowledged for conducting the extrusion coating trials and oxygen barrier measurements.

ORCID

Karoliina Helanto https://orcid.org/0000-0002-3604-2144
Riku Talja https://orcid.org/0000-0002-0760-4793
Orlando J. Rojas https://orcid.org/0000-0003-4036-4020

REFERENCES

[1] C. Andersson, *Packag. Technol. Sci.* **2008**, *21*, 339.
[2] V. Leminen, S.-S. Ovaska, P. Tanninen, J. Varis, *J. Appl. Packag. Res.* **2015**, *7*, 91.
[3] K. Helanto, L. Matikainen, R. Talja, O. Rojas, *BioResources* **2019**, *14*, 4902.
[4] Y. Cui, S. Kumar, B. Rao Kona, D. Van Houcke, *RSC Adv.* **2015**, *5*, 63669.
[5] PlasticsEurope, An analysis of European plastics production, demand and waste data. https://www.plasticseurope.org/en/resources/publications/1804-plastics-facts-2019 (accessed: November 2020)
[6] S. Amirabadi, D. Rodrigue, C. Duchesne, *Polym. Test.* **2018**, *68*, 61.
[7] T. Khuenkeao, N. Petchwattana, S. Covavisaruch, *AIP Conf. Proc.* **2016**, *1713*, 080005.
[8] W. Phetwarotai, D. Aht-Ong, *J. Therm. Anal. Calorim.* **2016**, *126*, 1797.
[9] G. Zou, Q. Jiao, X. Zhang, C. Zhao, J. Li, *J. Appl. Polym. Sci* **2015**, *132*, 41367.
[10] H. Moustafa, N. El Kissi, A. Abou-Kandil, M. Abdel-Aziz, A. Dufresne, *ACS Appl. Mater. Interfaces* **2016**, *9*, 20132.
[11] Y. Qin, J. Yang, M. Yuan, J. Xue, J. Chao, Y. Wu, M. Yuan, *J. Appl. Polym. Sci.* **2014**, *131*, 596.
[12] S. Jain, M. Misra, A. Mohanty, A. Ghosh, *J. Polym. Environ.* **2012**, *20*, 1027.
[13] F. Yu, T. Liu, X. Zhao, X. Yu, A. Lu, J. Wang, *J. Appl. Polym. Sci.* **2012**, *125*, E99.
[14] G. B. Kaggwa, L. Huynh, J. Ralston, K. Bremmell, *Langmuir* **2006**, *22*, 3221.
[15] A. Ghassemi, S. Moghaddamzadeh, C. Duchesne, D. Rodrigue, *J. Plast. Film Sheeting* **2017**, *33*, 361.
[16] D. Battegazzore, S. Bocchini, A. Frache, *eXPRESS Polym. Lett.* **2011**, *5*, 849.
[17] A. Buzarovska, G. Bogoeva-Gaceva, R. Fajgar, *J. Polym. Eng.* **2016**, *36*, 181.
[18] T. Cipriano, A. Da Silva, T. Da Fonseca, A. Da Silva, A. De Sousa, G. Da Silva, M. Rocha, *Polimeros* **2014**, *24*, 276.
[19] L. Castillo, S. Barbosa, P. Maiza, N. Capiati, *J. Mater. Sci.* **2011**, *46*, 2578.
[20] N. Petchwattana, S. Covavisaruch, S. Petthai, *Polym. Bull.* **2014**, *71*, 1947.
[21] C. Lee, M. M. Pang, S. C. Koay, H. L. Choo, K. Y. Tshai, *SN Appl. Sci.* **2020**, *2*, 354.
[22] S. Jain, M. Reddy, A. Mohanty, M. Misra, A. Ghosh, *Macromol. Mater. Eng.* **2010**, *295*, 750.
[23] C. Courgneau, S. Domenek, R. Lebosse, A. Guinault, L. Averous, V. Ducruet, *Polym. Int.* **2012**, *61*, 180.
[24] H. Cheng, Y. Yang, S. Li, J. Hong, G. Jang, *J. Appl. Polym. Sci.* **2015**, *132*, 42472.
[25] R. Koppolu, J. Lahti, T. Abitbol, A. Swerin, J. Kuusipalo, M. Toivakka, *ACS Appl. Mater. Interfaces* **2019**, *11*, 11920.
[26] K. Lahtinen, P. Maydannik, P. Johansson, T. Kääriäinen, D. Cameron, J. Kuusipalo, *Surf. Coat. Technol.* **2011**, *205*, 3916.
[27] K. Lahtinen, P. Johansson, T. Kääriäinen, D. Cameron, *Polym. Eng. Sci.* **2012**, *52*, 1985.
[28] S. Ouchiar, G. Stoclet, C. Cabaret, V. Gloaguen, *Macromolecules* **2016**, *49*, 2782.
[29] C. Simões, J. Viana, A. Cunha, *J. Appl. Polym. Sci.* **2009**, *112*, 345.
[30] J. Correa, A. Bacigalupe, J. Maggi, P. Eisenberg, *J. Renewable Mater.* **2016**, *4*, 258.
[31] M. Kumar, S. Mohanty, S. K. Nayak, M. Rahail Parvaiz, *Bioresour. Technol.* **2010**, *101*, 8406.
[32] A. Teamsinsungvon, Y. Ruksakulpiwat, K. Jarukumjorn, *Polym.-Plast. Technol. Eng.* **2013**, *52*, 1362.
[33] M. Yousfi, S. Livi, A. Dumas, J. Crepin-Leblond, M. Greenhill-Hooper, J. Duchet-Rumeau, *J. Appl. Polym. Sci* **2014**, *131*, 40453.
[34] Y. Zhu, H. Ma, L. Tong, Z. J. Fang, *Zhejiang Univ., Sci., A* **2008**, *9*, 1614.
[35] V. Pandey, J. Maia, *J. Appl. Polym. Sci.* **2021**, *138*, 49716.
[36] W. Chow, Z. Ishak, U. Ishiaku, J. Karger-Kocsis, A. Apostolov, *J. Appl. Polym. Sci.* **2004**, *91*, 175.
[37] Y. Leong, M. Bakar, Z. Ishak, A. Ariffin, B. Pukanszky, *J. Appl. Polym. Sci.* **2004**, *91*, 3315.
[38] L. Castillo, O. López, C. López, N. Zaritzky, M. García, S. Barbosa, M. Villar, *Carbohydr. Polym.* **2013**, *95*, 664.

[39] L. Massey, K. In, *Permeability properties of plastics and elastomers, 2nd Ed: A guide to packaging and barrier materials*, Norwich, Elsevier Science & Technology Books **2003**.
[40] R. Tol, V. Mathot, G. Groeninckx, *Polymer* **2005**, *46*, 2955.
[41] S. Xiang, L. Feng, X. Bian, G. Li, X. Chen, *Polym. Test.* **2020**, *81*, 106211.
[42] K. Balani, V. Verma, A. Agarwal, R. Narayan, *In Biosurfaces: A Materials Science and Engineering Perspective*, John Wiley & Sons, Incorporated, Somerset **2015**.
[43] N. Toft, M. Rigdahl, *Int. J. Polym. Mater. Polym. Biomater.* **2004**, *53*, 809.
[44] S. Kalia, L. Avérous, *In Biodegradable and biobased polymers for environmental and biomedical applications*, Scrivener Publishing, Salem, Massachusetts **2016**.
[45] M. Evstatiev, S. Simeonova, K. Friedrich, X. Pei, P. Formanek, *J. Mater. Sci.* **2013**, *48*, 6312.

SUPPORTING INFORMATION

Additional supporting information may be found online in the Supporting Information section at the end of this article.

How to cite this article: K. Helanto, R. Talja, O. J. Rojas, *J Appl Polym Sci* **2021**, *138*(41), e51225. https://doi.org/10.1002/app.51225